



ELSEVIER

Contents lists available at ScienceDirect

Deep-Sea Research II

journal homepage: www.elsevier.com/locate/dsr2

Phytoplankton growth, grazing and production balances in the HNLC equatorial Pacific

Michael R. Landry^{1,*}, Karen E. Selph², Andrew G. Taylor¹, Moira Décima¹, William M. Balch³, Robert R. Bidigare⁴

¹ Scripps Institution of Oceanography, University of California at San Diego, La Jolla, CA 92093-0227, USA

² Department of Oceanography, University of Hawaii at Manoa, Honolulu, HI 96822, USA

³ Bigelow Laboratory for Ocean Sciences, POB 475, W. Boothbay Harbor, ME 04575, USA

⁴ Hawaii Institute of Marine Biology, University of Hawaii at Manoa, Honolulu, HI 96822, USA

ARTICLE INFO

Available online 19 August 2010

Keywords:

Phytoplankton growth

Grazing

Production

Microzooplankton

Mesozooplankton

Depth distribution

C:Chla ratio

ABSTRACT

We investigate the hypothesis that phytoplankton growth and grazing processes are strongly balanced in high-nutrient low-chlorophyll (HNLC) waters of the equatorial Pacific using euphotic-zone estimates of rates and biomass determined for 30 stations during EB04 (December 2004) and EB05 (September 2005). As predicted by the balance hypothesis, depth-averaged instantaneous rates of phytoplankton growth and grazing losses to micro- and mesozooplankton show a net growth difference of zero. Contemporaneous estimates of phytoplankton biomass and specific rates from flow cytometry, microscopy and taxon-specific accessory pigments allow determination of constrained production-consumption trophic balances for the phytoplankton community as a whole and for major component populations. The magnitude of growth-based production ($867 \text{ mg C m}^{-2} \text{ d}^{-1}$) is consistent with measured ^{14}C primary production, given methodological differences. 70% of production is utilized by protistan herbivores within the microbial community; 30% is consumed by mesozooplankton. Among picophytoplankton (*Prochlorococcus*, *Synechococcus* and small eukaryotes), representing 40% of community biomass and 27% of daily biomass growth, microzooplankton consume almost all production. Among groups of larger eukaryote taxa, including diatoms but dominated by dinoflagellate biomass, micro-grazers consume 51–62% of production, with the remainder available to mesozooplankton. Some leakage from the balance is expected as export of sinking phytoplankton cells and aggregates, but is constrained to no more than a few percent of daily production from alternate determinations of mesozooplankton grazing. The demonstrated balance of growth and grazing processes in the equatorial Pacific is inconsistent with recent claims from inverse models that a large flux associated with ungrazed picophytoplankton production dominates euphotic zone carbon export in the region.

© 2010 Elsevier Ltd. All rights reserved.

1. Introduction

The regulation of new production in high-nutrient low-chlorophyll (HNLC) areas of the eastern equatorial Pacific has been alternatively ascribed to general phytoplankton limitation by the trace element iron or to specific limitation of diatoms by silicic acid (Dugdale et al., 1995, 2007; Coale et al., 1996a,b; Dugdale and Wilkerson, 1998). Despite lack of consensus on the hypothesized limiting resource, each explanation assumes a close coupling of phytoplankton growth and grazing losses to zooplankton to regulate community structure and to account for the near steady-state chemostat qualities of high growth rate and

low standing stock in the region (Morel et al., 1991; Frost and Franzen, 1992; Landry et al., 1997; Dugdale et al., 2011). The field evidence to date for a balance of growth and grazing rates has been supportive (e.g., Landry et al., 1997, 2003), yet limited and inconclusive. In addition, recent inverse model analysis of data from the US JGOFS EqPac (Joint Global Ocean Flux Studies, Equatorial Pacific) Program has suggested that the direct and indirect contributions of picophytoplankton to carbon export in the region may be quite large ($149 \text{ mg C m}^{-2} \text{ d}^{-1}$), associated with a large flux of picophytoplankton production that escapes grazing by protistan consumers (Richardson et al., 2004). If that is so, then efficient cropping of picophytoplankton within the microbial food web, a central tenet of grazer regulation of community composition, cannot be true, and much of what we think we know about phytoplankton control mechanisms in the equatorial Pacific would be in doubt.

* Corresponding author. Tel.: +1 858 534 4702; fax: +1 858 534 6500.
E-mail address: mlandry@ucsd.edu (M.R. Landry).

Data from the EB04 and EB05 cruises in the equatorial Pacific in December 2004 and September 2005 allow a rigorous analysis of the growth-grazing balance, with euphotic-zone integrated rates of phytoplankton growth (μ , d^{-1}) and mortality losses to microzooplankton grazing (m , d^{-1}) and mesozooplankton grazing (M , d^{-1}) at 32 stations. The predicted mean balanced condition for the region ($\mu - m - M \approx 0$) can therefore be tested. Complementary assessments of phytoplankton biomass and rates from flow cytometry, microscopy and taxon-specific accessory pigments at 30 of the experimental stations also allow for the first time a well-constrained determination of carbon-based production and consumption for the community as a whole and for its major component populations. We use these budget determinations to elucidate trophic controls and food-web fluxes in the HNLC equatorial Pacific.

2. Materials and methods

2.1. Cruise plan and sampling routine

We conducted our study in the equatorial Pacific between 110 and 140°W on two cruises of the R/V *Roger Revelle*. For EB04 (December 2004), we first sampled at 110°W from 4°N to 4°S at 1° spacing, followed by an east-west transect along the equator from 115° to 140°W. For EB05 (September 2005), the initial sampling was done from 4°N to 2.5°S at 140°W, followed by a west-east transect at 0.5°N from 140° to 123.5°W.

At each station, we collected seawater at 8 depths in the euphotic zone corresponding to light levels of 0.1, 0.8, 5, 8, 13, 31, 52 and 100% of incident solar irradiance (I_0). Samples of the water at each depth were used to assess microbial community abundance and biomass (Taylor et al., 2011) and to determine the rates of phytoplankton growth and microzooplankton grazing (Selph et al., 2011), and ^{14}C primary production (Balch et al., 2011). At mid-day (1000–1100) and mid-night (2200–2300), we also towed a plankton net obliquely through the euphotic zone to determine mesozooplankton biomass and gut-fluorescence estimates of grazing (Décima et al., 2011). The studies cited above comprise the primary sources of biomass and rate data for this study, and hence present detailed accounts of the methods, results and interpretations. In the sub-sections below, we provide brief overviews of the analytical and experimental methods that are relevant to our synthesis of the data.

2.2. Microplankton community analyses

Abundance, biomass and composition of the microbial community were analyzed by flow cytometry (FCM), microscopy, and pigments (HPLC, high-performance liquid chromatography). Selph et al. (2011) give details of the HPLC and FCM protocols. Taylor et al. (2011) present details of the methods used for microscopical analyses.

Samples (1.2–2.3 L) for HPLC analyses were filtered onto 25-mm GF/F filters, wrapped in foil, frozen in liquid nitrogen and stored at $-80^\circ C$. Laboratory analyses followed Bidigare et al. (2005). Pigments were extracted in 3 ml of 100% acetone for 24 h (dark, $0^\circ C$), with canthaxanthin added as an internal standard. After centrifuging to remove cell debris, subsamples were injected into a Varian 9012 HPLC system with absorption detectors at 436 and 450 nm. Pigment peaks were identified by retention times relative to pure standards and algal extracts of known composition.

FCM samples (2 ml) were preserved with 0.5% paraformaldehyde, frozen in liquid nitrogen and stored at $-80^\circ C$. Thawed

samples were stained with Hoechst 33342 ($1 \mu g ml^{-1}$) in the dark for 1 h and analyzed using a Beckman-Coulter EPICS Altra flow cytometer with dual lasers (1 W at 488 nm; 200 mW in UV) and a syringe pump for volumetric sample delivery. Calibration beads (yellow-green 0.5 and 1.0 μm ; UV 0.5- μm) were used as fluorescence standards. For the present analyses, we distinguished populations of *Prochlorococcus* (PRO), *Synechococcus* (SYN) and small photosynthetic eukaryotes (P-Euk) by their different fluorescence and light-scattering signatures. PRO and SYN abundances were converted to biomass estimates using factors of 32 and 101 fg C cell $^{-1}$, respectively (Garrison et al., 2000).

Biomass assessments for single-celled autotrophic and heterotrophic eukaryotes (protists) were made by digitally-enhanced epifluorescence microscopy (EPI) on two slide preparations, after freezing and storage at $-80^\circ C$. Cells $< 10\text{-}\mu m$ in size were enumerated in 50-ml aliquots preserved with paraformaldehyde (0.5% final concentration), stained with proflavin (0.33% w/v) and DAPI ($10 \mu g ml^{-1}$) and mounted onto black 0.8- μm black Nuclepore filters. Larger cells were enumerated on 500-ml subsamples, preserved according to Sherr and Sherr (1993), stained with proflavin and DAPI, and mounted onto 8- μm black Nuclepore filters. The slides were imaged and digitized at $630 \times$ (50 ml) or $200 \times$ (500 ml) using a Zeiss AxioVert 200M microscope with an AxioCam HR color CCD digital camera. Cell biovolumes (BV; μm^3) were determined from length (L) and width (W) measurements using the formula for a prolate sphere ($BV = 0.524LWH$), where cell height (H) on the filters was empirically determined to be 0.5W for naked flagellates (including dinoflagellates). Carbon (C; pg cell $^{-1}$) biomass was computed from BV from the equations of Menden-Deuer and Lessard (2000): $C = 0.216BV^{0.939}$ for non-diatoms, and $C = 0.288BV^{0.811}$ for diatoms.

For 8 stations on the EB04 cruise, samples (250 ml) fixed with 5% acid Lugol's solution were analyzed for biomass of ciliates, which were sub-optimally preserved and rarely counted on the slides. Subsamples of 100 ml were settled in Utermöhl sedimentation chambers for at least 24 h and counted and measured with a Zeiss inverted microscope. To convert cell biovolume estimates to carbon, we used $0.19 \mu g C \mu m^{-3}$ for naked ciliates (Putt and Stoecker, 1989) and $C (pg) = 44.5 + 0.053 \text{ lorica volume } (\mu m^3)$ for loricate ciliates (Verity and Langdon, 1984).

2.3. Rates of phytoplankton growth and grazing mortality

Experimental studies of phytoplankton growth and microzooplankton grazing were conducted at each station (Selph et al., 2011) using the two-treatment dilution approach (Landry et al., 1984, 2008). Water was collected in the early morning (0300–0400) using a CTD-rosette system with acid-cleaned 10-L PVC Niskin bottles with Teflon-coated springs. This was the same hydrocast and the 8 sampling depths used for measurements of community biomass described above, which became the initial time-point estimates of community standing stock for the experimental incubations (Selph et al., 2011; Taylor et al., 2011). For each depth, one 2.8-L polycarbonate bottle was filled with whole seawater while a second bottle received a measured 1.8 L volume of filtered (0.1- μm) seawater from the same depth before being topped up gently with whole seawater (total volume ~ 2.8 L). The bottles were incubated for 24 h in seawater-cooled shipboard incubators corresponding to the relative light levels (% I_0) of the depth of collection. Final samples were taken for HPLC, FCM and EPI analyses.

For each parameter measured (total chlorophyll *a*, taxon-specific accessory pigments and FCM populations), instantaneous

rates of phytoplankton growth (μ , d^{-1}) and microzooplankton grazing (m , d^{-1}) were estimated from initial and final standing stocks. Assuming a linear decline in grazing mortality with dilution, as confirmed with full dilution experiments on this and previous studies in the region (Landry et al., 1995a,b, 2000, in review; Verity et al., 1996), the net rate of change (k) of a measured parameter is $k = \mu - m$ in the undiluted bottles and $k_d = \mu - xm$ in diluted bottles, where “ x ” = the fraction of natural grazer density in the dilute treatment (0.37 in these experiments). The two equations are solved for the two unknowns, μ and m :

$$m = (k_d - k) / (1 - 0.37) \quad \text{and} \quad \mu = k + m.$$

To distinguish growth rates in cell biomass from pigment artifacts, growth rates based on changes in pigment concentrations were corrected using the ratios of HPLC pigments to biomass (microscopy or FCM) in initial and final samples (Selph et al., 2011). We used the change in C:Chl a from initial and final measurements to determine the unbalanced rate of pigment growth (relative to cell biomass) for the phytoplankton community. Similar initial/final corrections for pigment effects were made for individual populations by various approaches, such as the ratio of carbon to fucoxanthin for diatoms, the ratio of FCM red fluorescence (chlorophyll) per cell for *Prochlorococcus*, the ratio of 2–10 μ m eukaryote biomass to 19'-hexanoyloxyfucoxanthin for prymnesiophytes, and the ratio of 10–20 μ m autotroph biomass to peridinin for dinoflagellates. Mean rate corrections were calculated for each light level for the two cruises, then applied to individual station experiments at each light depth. At 0.1% I_0 , the correction was erratic for EB05 and poorly resolved for EB04. For community growth rate estimates at this depth, we consequently used the cruise-median correction for EB05 and none for EB04.

2.4. Phytoplankton production

We determined phytoplankton production rates by two approaches: 1) the net rates of ^{14}C -uptake into particles, and 2) the computed product of biomass and growth rates from dilution incubations. The ^{14}C methods and detailed results are presented by Balch et al. (2011). Water samples for these experiments were taken at 6 light depths (52, 31, 13, 5, 0.8 and 0.1% I_0) from 12-L GO-FLO bottles on a trace-metal clean rosette sampler. This cast was done immediately after the CTD-rosette sampling for community biomass and dilution experiments (typically 0400–0500), and the ^{14}C incubations, in 250-mL polycarbonate bottles, were conducted for 24 h under identical conditions as the dilution experiments. Samples were filtered onto 0.4- μ m polycarbonate filters and analyzed according to Balch et al. (2000).

Carbon-based estimates of phytoplankton community production (PP) and microzooplankton grazing (PG) were calculated using growth (μ) and grazing (m) rates based on total chlorophyll a (TChl a) from dilution experiments and the following equations from Landry et al. (2000):

$$PP = \mu C_0 (e^{(\mu-m)t} - 1) / (\mu - m)t, \quad \text{and}$$

$$PG = m C_0 (e^{(\mu-m)t} - 1) / (\mu - m)t$$

where C_0 is initial autotrophic carbon biomass in $mg\ C\ m^{-3}$ and t = time (1 day). Similarly, taxon-specific estimates of carbon production and grazing were calculated for all components of the community where parameter estimates of μ and m could be reasonably associated with a C-based estimate of standing stock. For example, production rates of *Prochlorococcus* (PRO), *Synechococcus* (SYN) and diatoms were determined from initial (C_0) biomass estimates for each of these groups and rate assessments from divinyl chlorophyll a (DVChl a), FCM cell counts

(PRO and SYN), and fucoxanthin (FUCO), respectively. Production rates of eukaryotes other than diatoms (i.e., Other Euks) were computed from rate estimates based on monovinyl chlorophyll a (MVChl a) and total biomass of all MVChl a containing autotrophs (=Total C - PRO). After total production of MVChl a taxa was determined, the production rates of diatoms and SYN were subtracted to yield the contribution of Other Euks by difference.

The eukaryote assemblage was further subdivided into production contributions from autotrophic dinoflagellates (A-Dino) and prymnesiophytes (Prymn) based on microscopical estimates of their standing biomass and rate determinations from the pigments peridinin (PER) and 19'-hexanoyloxyfucoxanthin (HEX), respectively. For Prymn, we used relationships between carbon biomass and HEX established for each of the light depths from EB04 to estimate carbon from HEX on EB05 (Prymn was not distinguished microscopically from other flagellates on this cruise). After biomass of A-Dino and Prymn was subtracted from total flagellate carbon, the remainder was divided among other groups based on relative contribution to the remaining unassociated accessory pigments. Pelagophyte (Pelago) production was estimated from rates based on 19'-butanoyloxyfucoxanthin (BUT). Since pigment signals for other groups were too weak for rate analyses, we used flow cytometrically determined rates for small eukaryote cells (P-Euk) to compute production for the remaining biomass. Based on pigments, prasinophytes comprised most of this biomass, so the cells in this category were assumed to be small green forms, possibly *Ostreococcus* spp.

All production rate calculations were made for each incubation light depth at each station separately; then they were vertically integrated by the trapezoidal method for the full euphotic zone at each station. Error estimates are for the means of the separate depth-integrated determinations at the 30 sampling stations.

2.5. Mesozooplankton grazing estimates

We used a 1-m² ring net with 202- μ m Nitex mesh for mesozooplankton collections (Décima et al., 2011). The net was towed obliquely for 20 min at a ship speed of 1–2 kts (2–4 $km\ h^{-1}$), with a General Oceanics flowmeter recording volume filtered and a Vyper Suunto dive computer recording tow depth and duration. On recovery, the contents of the cod end were anesthetized with carbonated water to prevent gut evacuation (Kleppel and Pieper, 1984), then size-fractionated, concentrated onto 47-mm GF/F filters and frozen ($-80\ ^\circ C$) for later processing (Décima et al., 2011).

Pigments were extracted in replicate 1/8 sections of the filters in 90% acetone using a tissue grinder, and the homogenate was centrifuged before the concentration was measured fluorometrically (Strickland and Parsons, 1972). Euphotic zone estimates of gut phaeopigment concentration (GPC, $mg\ Phaeo\ m^{-2}$) were computed from sample concentration, the fraction of net tow analyzed, the depth of tow and the volume of water filtered. In subsequent calculations, we used GPC estimates from the paired day-night tows at each station to average out the diel biases in grazing activity and vertical migration. For a few stations where paired day-night tows were not available, we estimated the missing tows using mean day:night ratios at other stations.

Daily instantaneous rates of phytoplankton mortality (M , d^{-1}) from mesozooplankton grazing were computed as

$$M = GPC \times 24K \times Chl_z^{-1}$$

where K (h^{-1}) is the gut evacuation rate constant of $2.1\ h^{-1}$ derived from shipboard gut experiments during the US JGOFS EqPac program (Zhang et al., 1995) and Chl_z is the depth-integrated concentration of Chl a in the euphotic zone ($mg\ Chl\ a\ m^{-2}$).

3. Results

3.1. Mean depth profiles

The general status of phytoplankton in the study region can be defined by the mean depth profiles of carbon biomass, C:Chla ratio, growth, grazing, and production rates (Fig. 1). The mean biomass ($\pm 95\%$ confidence limits) of phytoplankton is $19.0 \pm 2.3 \text{ mg C m}^{-3}$ in the upper euphotic zone, declining smoothly below the 10% light level to $< 5 \text{ mg C m}^{-3}$ at the 0.1% I_0 . C:Chla averages 78 ± 7.2 for the upper euphotic zone, with a slight maximum at 50% I_0 that drops off with decreasing light level to minimum values around the 1% light level. As noted by Taylor et al. (2011), the apparent increase in C:Chla in deeper waters is likely an artifact of applying a fixed relationship to convert cell biovolumes to carbon equivalents at all depths. The data suggest that the carbon density of recognizable cells in the lower euphotic zone is about 2/3rds that of healthier cells in the upper layers. Nonetheless, it is clear from the remaining panels of Fig. 1 that this potential problem in biomass measurement has a negligible impact on production estimates at the bottom of the euphotic zone because growth rates there are low.

Instantaneous growth rates (μ) of phytoplankton are depressed in incubations that experience unnaturally long exposure to high light (100% I_0). Elsewhere in the upper euphotic zone, where light appears saturating, phytoplankton have a broad growth maximum with rates on the order of $0.8\text{--}0.9 \text{ d}^{-1}$ (Selph et al., 2011). This is also reflected in calculated estimates of production rate (biomass growth), which average between 17 and $18 \text{ mg C m}^{-3} \text{ d}^{-1}$ for incubations between the light depths of 15 to 52% I_0 . Below this, rates of instantaneous growth and C production decline with diminishing light to values of zero at 0.1% I_0 . The rates of phytoplankton grazing mortality (m) and biomass consumption by microzooplankton follow the general shape of their corresponding growth rate profiles, but the curves are significantly offset at light depths above 1% I_0 . Production exceeds microzooplankton grazing losses by $6 \text{ mg C m}^{-3} \text{ d}^{-1}$ in the upper euphotic zone. The fate and composition of this excess growth are the core issues of the growth-grazing balance.

3.2. The growth-grazing balance

Given the overview of mean depth relationships, Table 1 now examines phytoplankton growth and grazing rate data at

individual stations. To conform to the constraints of the mesozooplankton rate assessments, which are based on integrated chlorophyll for the euphotic zone, all rates in this analysis are compared on the same basis, the euphotic zone mean values of μ and m being weighted to the depth distribution of TChla.

Table 1 shows clearly that the net balance between measured growth and grazing losses at individual stations is imperfect. There are interesting areas around the equator on EB04 (Stns. 7, 9, 16 and 18) where the net balance shows a substantial excess of growth over grazing ($> 0.1 \text{ d}^{-1}$). On the other hand, stations 9, 11 and 13 on EB05, also in the vicinity of the equator, show equally strong excess grazing over growth. Between cruises, mean phytoplankton growth rates were slightly higher during EB04 than EB05 ($0.47 \pm 0.16 \text{ d}^{-1}$ vs $0.41 \pm 0.11 \text{ d}^{-1}$, respectively), microzooplankton grazing rates were nearly identical ($0.31 \pm 0.13 \text{ d}^{-1}$ vs $0.32 \pm 0.10 \text{ d}^{-1}$, respectively), and mesozooplankton grazing was higher in 2005 ($0.12 \pm 0.04 \text{ d}^{-1}$ vs $0.16 \pm 0.07 \text{ d}^{-1}$, respectively). Of these, only the cruise differences for mesozooplankton grazing were statistically significant (Mann-Whitney U test, $p=0.05$, two-sided). From the measured station rates, the mean calculated net rates of change are slightly positive for EB04 ($0.03 \pm 0.08 \text{ d}^{-1}$) and slightly negative for EB05 ($-0.06 \pm 0.13 \text{ d}^{-1}$); however, 95% confidence limits for both overlap zero. Given the absence of dramatically different results for the different times and station locations sampled during the two cruises, the data are combined for subsequent analyses.

Overall, Table 1 documents a general balance among growth and loss rates, with a mean difference of essentially zero. Mean grazing by microzooplankton accounts for 70% of euphotic-zone integrated phytoplankton growth. Mesozooplankton consume the other 30% on average. This essentially means that the excess production depicted in the mean depth profiles of Fig. 1 comprises the primary food resource for mesozooplankton.

3.3. Microzooplankton grazing relationships

Figs. 2 and 3 examine the mortality and consumption rates ascribed to microzooplankton as a function of grazer biomass, considered in two ways. For a subset of the data, 8 stations from EB04, all components of the protistan microzooplankton were quantified microscopically, including biomass assessments of ciliates in Lugol's preserved samples. We call this biomass

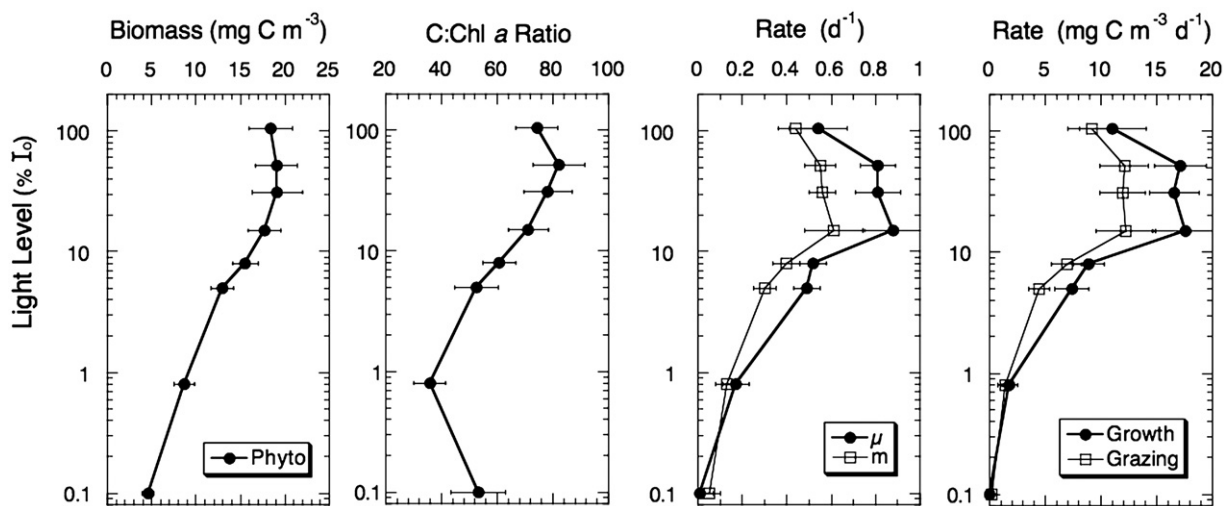


Fig. 1. Mean depth profiles for phytoplankton community carbon biomass, C:Chla ratio, and rate estimates from EB04 and EB05 cruises in the equatorial Pacific. Carbon biomass is from combined microscopy and flow cytometry (Taylor et al., 2011). Instantaneous rates of phytoplankton growth (μ) and grazing mortality from microzooplankton (m) are from dilution experiments (Selph et al., 2011). Production and microzooplankton grazing rates are computed from instantaneous rates and biomass. Error bars are 95% confidence intervals ($n=30$ stations).

category H-Protists (HP), and they provide the only data with which we can legitimately compare measured rates to measured biomass of all identifiable phagotrophic groups. For the full data comparison, we applied the mean 8-station estimates of ciliate biomass at each of the light depths to all stations where ciliates were unmeasured, and we further added half of the measured

Table 1

Growth-grazing balances for experimental stations in the eastern equatorial Pacific during EB04 (December 2004) and EB05 (September 2005) cruises. μ =phytoplankton growth rate; m =mortality rate to microzooplankton grazing; M =mortality rate to mesozooplankton grazing; $\text{Net}=\mu-(m+M)$. All rates are depth-integrated averages for the euphotic zone.

Exp	Date	Lat (°N)	Lon (°W)	μ (d ⁻¹)	m (d ⁻¹)	M (d ⁻¹)	Net (d ⁻¹)
1	11 Dec 04	4	110	0.15	0.09	0.12	-0.05
2	12 Dec 04	3	110	0.12	0.14	0.10	-0.13
3	13 Dec 04	2	110	0.33	0.22	0.09	-0.02
4	14 Dec 04	1	110	0.34	0.19	0.17	-0.02
5	15 Dec 04	0	110	0.45	0.20	0.07	0.18
6	16 Dec 04	-1	110	0.39	0.17	0.17	0.10
7	17 Dec 04	-2	110	0.37	0.23	0.11	0.03
8	18 Dec 04	-3	110	0.53	0.43	0.06	0.05
9	19 Dec 04	-4	110	0.37	0.23	0.08	0.06
10	21 Dec 04	0	116.7	ND	ND	0.10	
11	22 Dec 04	0	120	0.54	0.29	0.10	0.16
12	23 Dec 04	0	122.8	0.49	0.30	0.09	0.10
13	24 Dec 04	0	125.5	0.55	0.36	0.19	-0.01
14	25 Dec 04	0	128.2	0.66	0.42	0.16	0.08
15	26 Dec 04	0	131.6	0.65	0.45	0.14	0.06
16	27 Dec 04	0	135.2	0.63	0.47	0.13	0.02
17	28 Dec 04	0	138.7	0.64	0.49	0.11	0.04
18	29 Dec 04	0	140	0.45	0.37	0.19	-0.11
19	30 Dec 04	0	140	0.53	0.41	0.16	-0.05
20	10 Sept 05	4	140	0.32	0.18	0.10	0.04
21	11 Sept 05	2.5	140	0.45	0.27	0.11	0.07
22	12 Sept 05	1	140	0.40	0.21	0.24	-0.05
23	13 Sept 05	0.5	140	0.25	0.12	0.13	-0.01
24	14 Sept 05	0	140	0.32	0.31	0.16	-0.15
25	15 Sept 05	-0.5	140	0.30	0.32	0.27	-0.29
26	16 Sept 05	-1	140	0.34	0.46	0.17	-0.29
27	17 Sept 05	-2.5	140	0.51	0.40	0.04	0.07
28	20 Sept 05	0.5	132.5	0.56	0.29	0.13	0.14
29	21 Sept 05	0.5	130.2	0.49	0.43	0.22	-0.16
30	22 Sept 05	0.5	128	0.40	0.32	0.07	0.02
31	23 Sept 05	0.5	125.7	0.27	0.28	0.12	-0.13
32	24 Sept 05	0.5	123.5	0.54	0.43	0.21	-0.10
33	25 Sept 05	1.7	125	0.57	0.39	0.22	-0.04
	Mean			0.43	0.31	0.14	-0.01
	Stdev			0.14	0.11	0.06	0.11

biomass of the autotrophic flagellates (dominated by dinoflagellates) to represent the potential grazing contribution of mixotrophs feeding with about half of the uptake efficiency of pure heterotrophs (Stukel et al., 2011). This category, which we call Total Protistan Grazers (TPG), is an estimate of the maximum protistan biomass sustained by grazing on phytoplankton. Since any amount of mixotrophy by pigmented cells would only add to the total grazers, HP is consequently a minimum estimate of protistan grazer biomass.

Phytoplankton mortality due to microzooplankton grazing (m) is strongly ($p < 0.01$) related to both HP and TPG (Fig. 2). The slopes of the relationships are quite different, however, because the grazer biomass estimates are minimum-maximum extremes. The regression slope ($0.179 \text{ L } \mu\text{g C}^{-1} \text{ d}^{-1}$) for the minimum biomass estimate HP means that $1 \mu\text{g C L}^{-1}$ of HP biomass clears 179 mL of seawater d^{-1} of phytoplankton prey. The TPG regression slope sets the lower limit of biomass-specific clearance rate at $65 \text{ mL } \mu\text{g C}^{-1} \text{ d}^{-1}$. Both relationships show significant negative intercepts, and therefore imply zero grazing at positive values of grazer biomass. These low rates occur generally at the base of the euphotic zone where phytoplankton biomass decreases disproportionately relative to grazer biomass. They might therefore be indicative of a threshold concentration of prey below which grazing effort (clearance rate) declines (e.g., Strom et al., 2000).

The computed rate of carbon consumption by microzooplankton is also strongly ($p < 0.01$) related to protistan biomass (Fig. 3). The slopes of these relationships can be interpreted in terms of growth potential. Assuming a realistic gross growth efficiency (GGE) of 30%, for example, the slope ($4.0 \mu\text{g C } \mu\text{g C}^{-1} \text{ d}^{-1}$) means that HP consumes 400% of body C d^{-1} , which gives an implied growth rate of 120% of carbon mass d^{-1} , or an instantaneous growth rate (μ) of 0.79 d^{-1} . In contrast, phytoplankton consumption by TPG would be sufficient to support 46% of body carbon as daily growth, or $\mu = 0.38 \text{ d}^{-1}$. These numbers have meaning in a balanced system context if we consider that autotrophic and heterotrophic protists of broadly overlapping size, and therefore comparable vulnerabilities to size selective predators, must be able to sustain equivalent growth rates on average. For HP, the computed growth rate above is comparable to the mean maximum growth of phytoplankton in the upper euphotic zone (Fig. 1). For TPG, the computed growth rate is close to the mean depth-integrated rates for phytoplankton (Table 1). It is thus reassuring that estimates of herbivory alone, without invoking

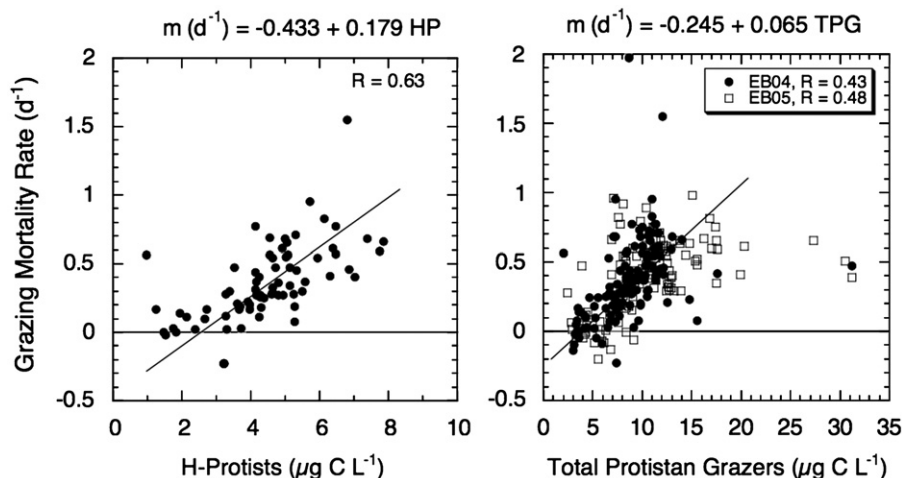


Fig. 2. Relationships between instantaneous rates of grazing mortality of microzooplankton and microzooplankton biomass determined as heterotrophic protists (H-Protists, HP) for 8 EB04 stations and estimates of Total Protistan Grazers (TPG), including mixotrophs, for all stations. Linear regression equations are Model II (reduced major axis) ($p < 0.01$).

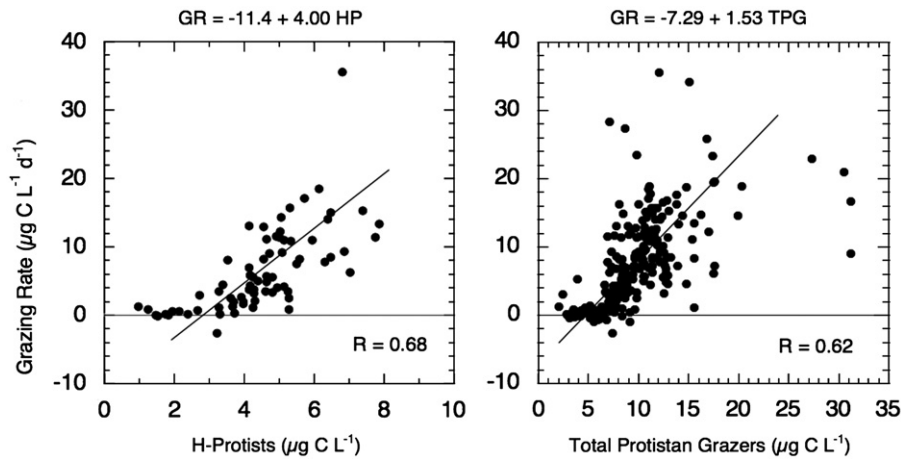


Fig. 3. Relationships between grazing rates of microzooplankton and microzooplankton biomass determined as heterotrophic protists (H-Protists, HP) for 8 EB04 stations and estimates of Total Protistan Grazers (TPG), including mixotrophs, for all stations. Linear regression equations are Model II (reduced major axis) ($p < 0.01$).

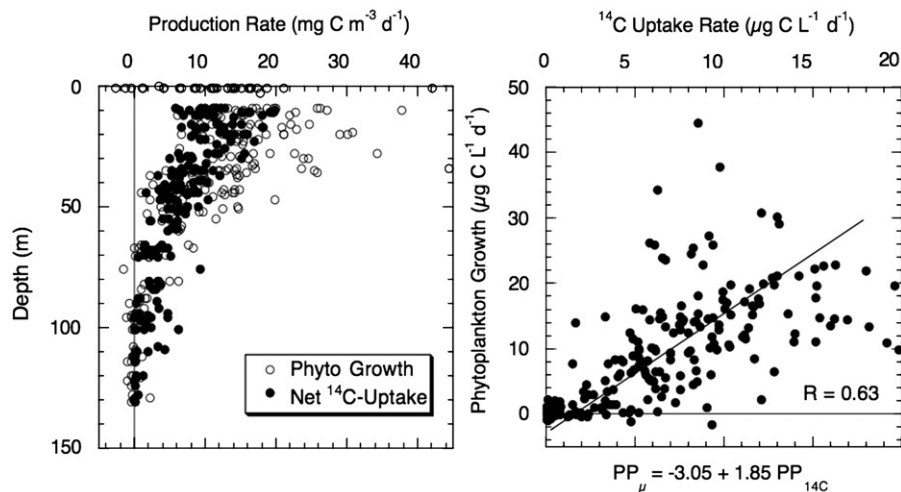


Fig. 4. Relationships between estimates of phytoplankton production determined from growth rates and biomass (growth) and standard 24-h primary production measurements from uptake of ^{14}C -bicarbonate into particles. Left panel shows depth profile of all data. Right panel is Model II linear regression of the two production values ($p < 0.1$).

consumption of H-bacteria, detritus or inter-guild feeding among H-protists, are in the range that would satisfy the growth rate constraint for autotrophs and heterotrophic protists in a balanced ecosystem.

3.4. Comparison of production rates

Fig. 4 compares the production rates calculated from biomass and rate estimates from dilution experiments to standard measurements of primary production by net ^{14}C -uptake into suspended particles. The two approaches show strongly overlapping distributions throughout the euphotic zone, though rate estimates based on the dilution approach are higher in the upper euphotic zone on average. The two rate estimates are significantly related ($p < 0.01$), with the Model II regression slope implying that individual rate assessments based on measured growth rate and biomass exceed ^{14}C rate estimates by 85%. Depth-integrated estimates are actually much closer, with mean estimates ($\pm 95\%$ confidence limits) for the former ($867 \pm 96 \text{ mg C m}^{-2} \text{ d}^{-1}$) exceeding the latter ($672 \pm 73 \text{ mg C m}^{-2} \text{ d}^{-1}$) by only 29%. We will consider the methodological reasons for why these rates should differ by about this amount in discussion. In the meanwhile, it is sufficient to note that the depth distributions and

integrated rates by these two methods are in reasonable agreement. Thus, the independent biomass assessments and the growth rate multipliers from dilution experiments that go into the production calculations must adequately reflect the mean stocks and rates in the system.

3.5. Taxon-specific production and grazing

Following from the overall balance observed in instantaneous rates of growth and grazing for the phytoplankton community (Table 1), here we examine how that applies to production processes, specifically, the partitioning of production and grazing fluxes among components of the phytoplankton community. Different taxa lend themselves to such an analysis with varying degrees of difficulty. *Prochlorococcus* and diatoms, for example, are relatively straightforward, each providing an easily identifiable population for biomass assessment and strong taxon-associated signals from FCM cell counts or HPLC pigments for rate determinations. Representing opposite ends of the phytoplankton community size spectrum, PRO and diatoms also show an interesting contrast in habitat discrimination in the equatorial Pacific, with high diatom production being strongly contained within the upper third (light-saturated portion) of the

euphotic zone, and the productivity maximum for PRO shifted much deeper (Fig. 5). Beyond photosynthetic bacteria (PRO and SYN) and diatoms, the rationales for biomass or rate assignments to other taxonomic groups become increasingly more tenuous. We have therefore organized this production analysis in two parts: those components that can be readily assigned (PRO, SYN, diatoms and Other-Euks), and those where assignments probably involve some group overlap and greater analytical uncertainty.

In the community balance, the grazing contribution of mesozooplankton is determined as the difference between biomass production of phytoplankton and consumption by microzooplankton. This follows reasonably from the demonstrated balance of instantaneous growth and loss rates in Table 1. Thus, in Table 2, mean ($\pm 95\%$ CL) production of $867 \pm 96 \text{ mg C m}^{-3} \text{ d}^{-1}$ is partitioned among grazers with 608 ± 79 and $260 \pm 70 \text{ mg C m}^{-3} \text{ d}^{-1}$ going to micro- and mesozooplankton, respectively. We independently computed the biomass flux to mesozooplankton using gut pigment estimates of the fraction of phytoplankton biomass consumed per day and station estimates of phytoplankton C biomass. The resulting grazing rate, $217 \pm 41 \text{ mg C m}^{-3} \text{ d}^{-1}$ is 17% lower than computed by difference, though well within the uncertainties of C:Chla conversions. Our gut pigment estimates implicitly assume the

mean C:Chla ratio at each station, but it is clear from the distribution of excess production in Fig. 1 (i.e., production – microzooplankton grazing) that mesozooplankton acquire food disproportionately from the upper euphotic zone where the C:Chla is significantly higher than average. We will revisit this point in discussion. To further develop the production analysis here, we take the reasonably good agreement between two estimates of mesozooplankton grazing as support for the calculation approach based on rate differences.

Among major groups, PRO and diatoms are about 4-fold different in terms of biomass (Table 2). However, they contribute equally to production, with almost all PRO production being consumed by micro-herbivores, while diatoms divide more evenly between micro- and mesozooplankton. SYN is comparable to diatoms in biomass, but produces 1/3rd the carbon, which is consumed by the microzooplankton. The remaining Other-Euks represent 58% of community biomass and contribute a comparable proportion to total community production. The majority (63%) of production in this mixed assemblage is consumed by microzooplankton. Among the major groups of phytoplankton, only PRO offers the potential for semi-independent assessments of production fluxes, sharing the same data on population biomass but using different instantaneous rate determinations from DVChla pigment analyses and from FCM cell counts (Selph et al., 2011). These two approaches give remarkably consistent estimates for microzooplankton grazing, and adequate agreement for production estimates. Interestingly, the average estimates for these approaches (153 and $145 \text{ mg C m}^{-3} \text{ d}^{-1}$ for production and microzooplankton grazing, respectively) give the best fit for the sum of the major groups (production = $864 \text{ mg C m}^{-3} \text{ d}^{-1}$; microzooplankton grazing = $602 \text{ mg C m}^{-3} \text{ d}^{-1}$) relative to the corresponding community totals. Within the major groups, therefore, the partitioning of biomass, production and grazing fates seem to be well resolved and tightly constrained.

Among the sub-groups of the Other-Euks category, the interpretations require more caution. The sum of the rate estimates for production ($443 \text{ mg C m}^{-3} \text{ d}^{-1}$) and microzooplankton grazing ($272 \text{ mg C m}^{-3} \text{ d}^{-1}$) fall short of the group totals (505 and $313 \text{ mg C m}^{-3} \text{ d}^{-1}$, respectively), which would imply that the instantaneous rates for computing fluxes are underestimated to some extent, or that the biomass is not apportioned accurately among groups. Even so, agreement of these numbers within 15% is a good result overall. We can reasonably make two observations from this portion of the analysis. First, dinoflagellates are the single most important contributors to all measured parameters – biomass, production, and grazing of both micro- and mesozooplankton. Second, the very small photosynthetic eukaryotes, possibly underestimated here as biomass, show a strong coupling of production to microzooplankton consumption similar to that of PRO and SYN. In effect, all of the instantaneous μ and m estimates derived from actual initial and final cell counts by flow cytometry show tightly constrained growth-grazing balances of picophytoplankton within the microbial food web.

4. Discussion

4.1. Reconciling ^{14}C production and phytoplankton growth

Before considering the implications of our results for food-web fluxes and export issues in the equatorial Pacific, we come back to the observation from Section 3.4 and Fig. 4 that dilution-based estimates of phytoplankton growth are significantly higher on average than ^{14}C estimates of primary production. It is important to understand, if not reconcile, these differences in order to

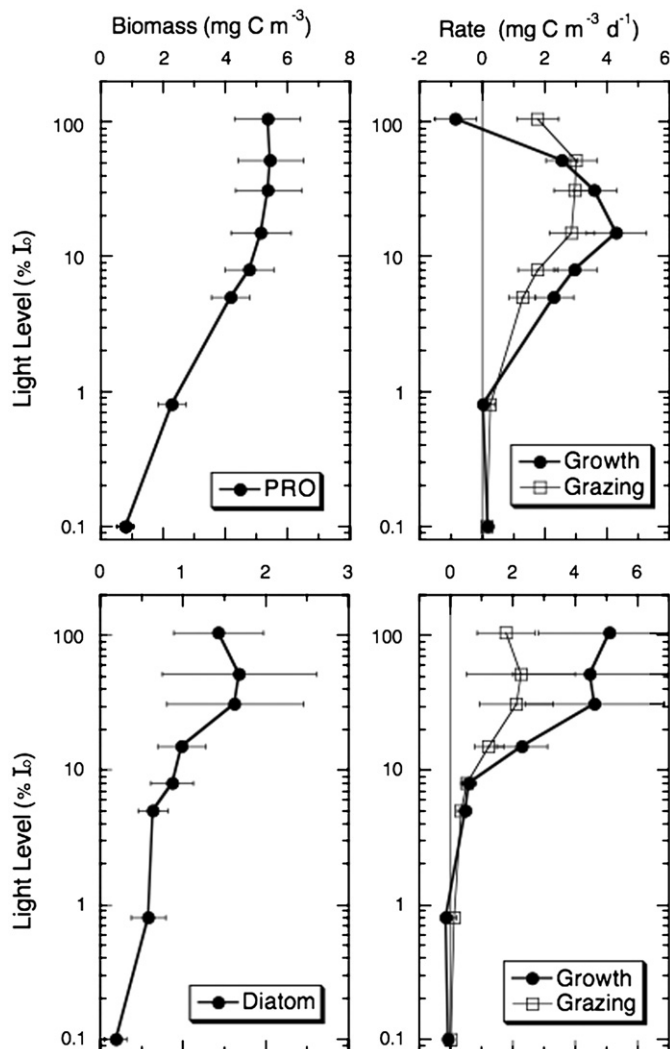


Fig. 5. Mean depth profiles of carbon biomass, production and microzooplankton grazing for *Prochlorococcus* (PRO) and diatoms from EB04 and EB05 cruises in the equatorial Pacific. Error bars are 95% confidence intervals ($n=30$ stations).

Table 2

Taxon-specific contributions to phytoplankton community biomass, production and grazing in the HNLC equatorial Pacific between 4°N–4°S, 110–140°W (EB04 and EB05 cruises). Estimates are means \pm 95% confidence limits for station profiles integrated to the depth of 0.1% surface irradiance. Total station number=30; full data were not available for experimental stations #1, 10 and 19 in Table 1. Biomass estimates are from assessments by microscopy and flow cytometry (Taylor et al., 2011). Rate estimates are based on dilution experiments with community and group-specific assessments by HPLC pigments, flow cytometry and microscopy (Selph et al., 2011). *Prochlorococcus* analyses are done with rates based both on the pigment DVChla and FCM cell counts. Mesozooplankton grazing estimates are computed as the difference between production and microzooplankton grazing assuming that average growth rates and grazing losses are in balance (Table 1). * = MesoZoo grazing determined independently from gut pigment analyses (Table 1), as % phytoplankton C biomass consumed d⁻¹.

Category	Biomass (mg C m ⁻²)	Production (mg C m ⁻² d ⁻¹)	Grazing (mg C m ⁻² d ⁻¹)	
			MicroZoo	MesoZoo
Total Phytoplankton	1385 \pm 93	867 \pm 96	608 \pm 79	260 \pm 70 *217 \pm 41
<i>Major Groups:</i>				
<i>Prochlorococcus</i> - DVChla	386 \pm 48	174 \pm 30	147 \pm 26	28 \pm 23
<i>Prochlorococcus</i> - FCM	386 \pm 48	132 \pm 21	143 \pm 24	-10 \pm 21
<i>Synechococcus</i>	107 \pm 18	50 \pm 8	58 \pm 11	-6 \pm 5
Diatoms	93 \pm 21	156 \pm 54	83 \pm 28	74 \pm 29
Other Eukaryotes	798 \pm 78	505 \pm 95	316 \pm 67	189 \pm 51
<i>Sub-groups of Other Eukaryotes:</i>				
Dinoflagellates	539 \pm 58	272 \pm 70	167 \pm 39	106 \pm 44
Prymnesiophytes	108 \pm 21	69 \pm 15	35 \pm 9	33 \pm 8
Pelagophytes	84 \pm 16	72 \pm 14	41 \pm 9	31 \pm 7
Other small eukaryotes	67 \pm 13	30 \pm 9	29 \pm 8	1 \pm 5

anchor our results to the constraints of a more traditional methodology.

The obvious problem with directly comparing these approaches is that the ¹⁴C method does not measure phytoplankton growth *per se*, but rather the net accumulation of ¹⁴C-labeled POC within the microbial community. Due to trophic processes and respiration, a significant fraction of the ¹⁴C-bicarbonate initially fixed as phytoplankton growth is respired to inorganic C as the incubation extends in time. Under conditions relatively similar to the present study in terms of community structure, phytoplankton growth, primary production and seawater temperature, for example, Dickson et al. (2001) found that 24-h depth-integrated estimates of ¹⁴C primary production in the Arabian Sea needed to be adjusted upward, on average, by 21% (range=11–30%, n=12) to account for metabolic losses relative to 12-h incubations terminated at sunset. Similar loss processes also occur during the initial 12 h (photoperiod), although the effect on rates is much smaller due to lower mean phytoplankton biomass and ¹⁴C specific activity during the day. Simply on the basis of carbon cycling, therefore, one should probably consider growth-based and 24-h ¹⁴C estimates of production to be in reasonable agreement if the former is 25–30% higher. As noted above, our depth-integrated estimates of phytoplankton C growth average 29% higher than contemporaneous rates of ¹⁴C-PP, which is in the range expected.

Algal mixotrophy is another reason to expect estimates of phytoplankton growth to exceed those from ¹⁴C-PP because bicarbonate uptake is not always the exclusive source of carbon for growth. Stukel et al. (2011) provides evidence from uptake of fluorescently labeled bacteria (FLB) that chlorophyll-containing cells accounted for about half of nanoplankton predation on bacteria in our study area, and we have shown here that accounting for mixotrophic grazers produces results consistent with the balanced system expectation that pigmented and non-pigmented protists of comparable size grow at similar rates. The extent to which unlabelled POC contributed to the nutrition and growth of phytoplankton in our experiments is an open issue, as mixotrophy may function more as a mechanism for scavenging growth-limiting trace elements (e.g., Fe) rather than a large amount of carbon. The relatively close agreement between our growth-based estimates of carbon production and the respiration/cycling correction for 24-h estimates of ¹⁴C-PP would seem to

suggest that acquired C from mixotrophy contributes only modestly to phytoplankton growth in the equatorial region. This is consistent with the conclusion of Stukel et al. (2011) that the mixotrophic strategy of small bacterivores serves mainly to acquire nutrients.

To be complete in terms of potential reasons for the production rate difference, we note that ¹⁴C-PP incubations were prepared with water collected from the trace metal clean rosette system. The dilution incubations were not, although we endeavored to use appropriate clean methods for handling bottles, processing water, etc. Previous work in the region has shown a rapid response of pigments to purposeful Fe fertilization or inadvertent Fe contamination, but little to no biomass or rate effects through at least the first day (Sanderson et al., 1995; Landry et al., 2000). These prior results, as well as the good agreement in expected versus observed production differences for ¹⁴C-PP, suggest that contamination artifacts play a minor to negligible role in our analyses.

4.2. Food-web balance constraints in the HNLC equatorial Pacific

Previous studies have invoked the grazer-balanced food web concept to explain the relative steady-state characteristics of the HNLC equatorial Pacific, including regulation of rapid growth and community structure under Fe or Si limitation (Frost and Franzen, 1992; Landry et al., 1997; Dugdale et al., 2011). The direct field evidence for such a mechanism has been supportive, but limited. Landry et al. (1997) found, for example, that the combined mean mortality rates attributable to micro- and mesozooplankton grazers balanced growth rate closely during the 1992 El Niño portion of the US JGOFS EqPac study. However, advective processes during the normal upwelling portion of EqPac moved excess growth of 0.16 d⁻¹ away from the equatorial divergence region, where its eventual fate was undetermined. During French JGOFS studies at 180° in 1995, a reasonably good balance of process rates was also seen (Landry et al., 2003; LeBorgne and Landry, 2003), but this study only involved a total of 8 rate experiments, at two stations with 2 depths each. The present study was designed specifically to assess food web balance and flux issues and brings together for the first time a well-coordinated suite of biomass and rate measurements extending

over the full euphotic zone at a large number of stations. One can always speculate that the results may have been different if the experiments had been conducted in different years, times of year or locations, and indeed future work may show interesting perturbations or temporal trends relative to our base survey. Ignoring this broad caveat, however, the general conclusions from our analysis are clear in many respects.

Overall, strong community-level balances are observed in the mean station estimates of net instantaneous rates (Table 1) and in the group-specific distributions of production and grazing fluxes (Table 2). Production estimates are consistent, given known methodological issues, with ^{14}C estimates of primary production. Biomass and grazing rate estimates for the microzooplankton are consistent with the growth rate constraint for balanced trophic fluxes of autotrophic and heterotrophic protists. Balch et al. (2011) have noted similar evidence for an overall system steadiness of system, citing a finely regulated balance of calcite production to ^{14}C -PP in their experimental data. It is important to note that the growth-grazing balance demonstrated here is net of other processes, such as viral-induced mortality or programmed cell death (e.g., Bidle and Falkowski, 2004; Baudoux et al., 2007; Franklin et al., 2006), which function essentially as closed loops of phytoplankton production to DOC. Such processes affect equally the populations in diluted and non-diluted treatments and are, therefore, invisible to the dilution incubation technique that was used here for population growth rate assessments.

Within the smallest size class of primary producers, basically the populations (PRO, SYN and P-Euks) readily enumerated by flow cytometry and typically referred to as pico- or ultraphytoplankton, dynamics are defined to first order by the direct coupling of growth and production to grazing losses within the microbial community. Realistically, there must be fluxes to known mesozooplankton consumers of bacterial-sized particles, such as appendicularians (Scheinberg et al., 2005), and some aggregate-associated export as well. The uncertainties in production and grazing estimate for PRO, derived from FCM and HPLC rate determinations (Table 2), suggest that these alternate fates could comprise an average of 5% up to as much as 16% (DVChla rates) of PRO production, or 8–28 $\text{mg C m}^{-2} \text{d}^{-1}$. PRO is the major component of the picophytoplankton, and including SYN and pico-eukaryotes from Table 2 does not increase our estimate of the amount of total picophytoplankton production that is ungrazed by protists, though there may clearly be times or locations when their contributions are significant. If one were to try to fully resolve the alternate fates of picophytoplankton, this magnitude of flux is large enough to be potentially measurable in designed feeding experiments with mesozooplankton or in direct observations of sinking into sediment traps, and they may well be ecologically important even though they represent a small portion of the total carbon budget for picoplankton in our data. However, the inverse model of Richardson et al. (2004) predicts a much larger flux of picophytoplankton production that is ungrazed by protists. For the four major EqPac cruises, their values for this flow (#24 in Table 1; Richardson et al., 2004) average 281 $\text{mg C m}^{-2} \text{d}^{-1}$, which exceeds our highest estimate of ungrazed picophytoplankton by an order of magnitude, and even surpasses our estimate of total primary production by all component populations of the picophytoplankton (214–254 $\text{mg C m}^{-2} \text{d}^{-1}$; Table 2). Picophytoplankton production that escapes protistan grazing control in the microbial food web is, in fact, one of the largest fluxes in the Richardson et al. (2004) model and the main driver of the very high contributions of picophytoplankton production to system export proposed by Richardson and Jackson (2007).

Resolving the picophytoplankton contribution to export requires quantification of all of the direct and indirect pathways

of carbon flow in a network analysis like Richardson and Jackson's (2007), which is beyond the scope of the present study. Nonetheless, our well-constrained field data suggest strongly that the production basis for high picophytoplankton contribution to export flux is grossly exaggerated in the Richardson et al. (2004) representation of carbon flows in the equatorial Pacific. Our data indicate that picophytoplankton comprise on the order of ~24–29% of total primary production (Table 2), whereas Richardson et al. (2004) suggest they comprise 85% of the total, on average. The latter estimate is based solely on the assumption that production is distributed according to size-fractionation of Chl *a*, which can be heavily biased toward smaller size fractions by the extrusion of flexible larger cells and cell fragments (e.g. chloroplasts) through 2- μm filter pores. Therefore, quite aside from the high fraction of picophytoplankton production that Richardson et al. (2004) propose escapes consumption in the microbial food web, our measured production rates do not support the assumption that Richardson et al. (2004) made to partition primary production among phytoplankton size classes. Landry (2009) has noted that similar inverse model results pointing to extraordinary export contributions of picophytoplankton in the Arabian Sea (Richardson et al., 2006) are attributable in part to this same assumption, and are likewise at odds with the strong database of microscopical biomass assessments of phytoplankton for that region (Garrison et al., 2000).

Among the major groups of plankton analyzed, PRO and diatoms provide an interesting contrast ecologically. PRO is a system dominant, accounting for 36% of TChla (Selph et al., 2011) and 28% of carbon biomass (Taylor et al., 2011), yet it grows slower than the community average and makes a disproportionately small contribution to production (18%). Diatoms, on the other hand, are a minor portion of biomass (7%) but the fastest growing group, and thus make a disproportionately large contribution to production (18%). That these two groups end up essentially equal in terms of system productivity is a bit surprising, although it supports the claim that diatoms are substantially more important as system drivers than their low biomass might indicate (Dugdale et al., 2007, 2011).

The issue of fast growing diatoms in an iron- or silicate-limited HNLC system is curious, yet consistent with previous studies (Latasa et al., 1997; Landry et al., 2003). One potential explanation is that the dominant diatom types in the region, long slender pennates with substantial vacuoles, are designed with relatively high surface area to carbon ratios to compete with other tiny cells for the limiting dissolved nutrients. The production profiles for diatoms, showing sharply decreasing rates below 30% of surface light intensity (Fig. 5), may also provide another important clue on this issue. PRO does less well near the surface, exhibiting a subsurface growth rate and production maximum, which agrees with previous inferences about PRO cell division rates based on cell cycle analysis in the equatorial region (depth maximum at 30 m; Vaultot et al., 1995). Our production depth maximum for PRO averages 33 m.

In a previous study of a mesoscale cyclonic eddy off Hawaii, we have described a diatom-dominated bloom with high biomass and growth rates deep in the euphotic zone where nutrients are available from uplifted isopycnals (Landry et al., 2008). PRO dominated the upper euphotic zone, above the diatoms, in this case. Based upon these two observations, there are clearly no rules that define the vertical habitat partitioning of PRO and diatoms in the tropical open ocean, or that preclude diatoms from growing well at moderate to low light levels, say 10% I_0 . However, production of equatorial diatoms seems to be virtually shut down at this light intensity in our experiments (Fig. 5). In addition, diatom production remains closely associated with the upper mixed layer even at the equator although upwelling from deeper waters is

generally regarded to be the main source of Fe and Si to the euphotic zone (Coale et al., 1996a). The distributions make more sense if we consider mechanisms that may enhance the flux of Fe near the surface. Atmospheric deposition is one, with the rate of Fe delivery being modest and likely irregular (episodic). Photo-oxidation of organically complexed Fe (Johnson et al., 1994) is another mechanism that may provide a steadier source of available Fe to the upper mixed layer under bright equatorial sunlight. Regardless, diatoms only benefit disproportionately from such processes by having unusual capabilities for uptake and storage (e.g., Marchetti et al., 2009) when they encounter patches of enhanced concentration.

While diatoms and PRO are extremes in many respects, the majority of the production fate for both is to grazing by microzooplankton. This is an important point for ecosystem modeling, which often assumes that diatoms are exclusively the prey of mesozooplankton. Dinoflagellates, in particular, as well as large ciliates, are efficient consumers of diatoms (Sherr and Sherr, 2007), and they were the grazers that responded to and eventually controlled the bloom of small pennate diatoms in IronEx II (Landry et al., 2000). If such ubiquitous consumers do not account for the bulk of grazing impact on rapidly growing diatoms, too much will be required from mesozooplankton to make up the difference. In this regard, it may be usefully observed that proportion of diatom production that escapes consumption by microzooplankton (47%) is not wildly different than the percentage for other eukaryotes (37%), which comprise the bulk of community biomass and production. This difference may mean that 10% of diatom production, a relatively small amount ($16 \text{ mg C m}^{-2} \text{ d}^{-1}$) in the community production balance, could be lost to direct export (sinking) from the euphotic zone. Alternatively, the concentration of diatom production in the upper euphotic zone may allow diatoms to be cleared more efficiently from the water column by mesozooplankton than the more broadly distributed other eukaryotes.

4.3. Phytoplankton export: a leaky balance?

As noted above, our data are not consistent with 1) the very high proportion (85%) of total primary production attributable to picoplankton and 2) a large portion of that production escaping protistan grazing that underlie Richardson and Jackson's (2007) claim that picophytoplankton dominate as the source material for C export in the equatorial Pacific. Despite this, it is undeniably the case that some living phytoplankton, including picoplankton, is exported from the euphotic zone, as individual cells, as the filtered but unconsumed contents of discarded appendicularian houses, and perhaps most importantly as particles attached to sticky (diatom) aggregates. During EqPac benthic sampling in 1992, for example, fresh phytodetritus was observed to blanket the seafloor at 4300–5000 m depth over a broad latitudinal band around the equator (Smith et al., 1996). Direct sinking export of phytoplankton is therefore an observed phenomenon in the region, not just a possibility. The mechanisms and magnitude, however, are unresolved.

A slow leakage of direct phytoplankton export from the euphotic zone is not precluded by our confirmation of a general growth-grazing balance. In the present analysis, we found that mesozooplankton consumption of phytoplankton determined from gut fluorescence and C:Chla ($217 \pm 41 \text{ mg C m}^{-2} \text{ d}^{-1}$) was slightly less than that implied from the difference of production and microzooplankton grazing ($260 \pm 70 \text{ mg C m}^{-2} \text{ d}^{-1}$; Table 2). As previously noted, this difference would be negligible if the calculations assumed that the applicable C:Chla was the mean of the mixed layer (78), rather than the mean of the water column

(64); that is, $217 \times 78/64 = 264 \text{ mg C m}^{-2} \text{ d}^{-1}$. Nonetheless, even if we assume that the difference between the two mesozooplankton grazing rate estimates, $43 \text{ mg C m}^{-2} \text{ d}^{-1}$, represents an unresolved portion of the balance that can be attributed to cell sinking, then the rate of cell loss is still relatively small – about 3% of standing stock lost per day, or ~5% of daily production. Similarly, the amount of phytodetritus observed on the seafloor during EqPac, while visibly impressive, was quantified at $31 \pm 15 \text{ mg C m}^{-2}$ (Smith et al., 1996), less than 4% of one day's worth of phytoplankton growth in the overlying euphotic zone.

While the estimates above would appear to set an upper limit to the magnitude of the export rain from phytoplankton sinking at a few % of phytoplankton production, the rate may be locally concentrated or perhaps substantially enhanced under some physical conditions. For example, while direct measurements of Chl *a* fluxes into short-term sediment traps deployed directly beneath the euphotic zone indicated very low losses to cell sinking during EqPac (Landry et al., 1997), during the normal upwelling phase of the study following the 1992 ENSO, a significant amount of phytoplankton growth (20%) was observed to escape contemporaneous losses to grazing and advect laterally away from the equator. The net accumulation of biomass from this mechanism formed a thin line of high concentration at a convergent front observed at 2°N, 140°W (Archer et al., 1997), which was also visible in satellite images extending for several hundred kilometers (Yoder et al., 1994). Such areas could be natural sites of intense resource depletion, TEP (transparent exopolymer particle) production, enhanced particle-particle interaction, and aggregate formation (Jackson, 1990; Alldredge and Jackson, 1995). In this particular case, the line was defined by a thin surface layer of large buoyant diatoms (*Rhizosolenia* spp.), which were prominent also in the seafloor phytodetritus (Smith et al., 1996).

In addition to being likely areas of high aggregate formation, subduction features associated with convergent fronts and the vortices of tropical instability waves (TIW) could be sites of mass export of particles and production from surface waters. Balch et al. (2009) have demonstrated large-scale subductive export of an initial 1-km surface patch of chalk particles into thin layers extending over 10's of kilometers. If subduction areas are disproportionately important for carbon export in the equatorial Pacific and particularly if their presence enhances the regionally averaged export by a significant amount, this needs to be known to model accurately the system response to climate variability. The relative magnitudes of fluxes in these areas are however difficult to assess from the normal way in which processes are studied on ocean research cruises at fixed stations that are physically disconnected with one another. We need rather to be able to track and quantify the origins, net accumulation and ultimate fate of production as it enters and moves through such features. Lagrangian-designed experimental studies (e.g. Landry et al., 2009) that focus on the export enhancement potential of physical features (fronts and TIW) are an important next step for understanding export mechanisms in the equatorial Pacific as well as reconciling the general balance of growth and grazing process in the upper water column against better resolved estimates of phytoplankton production leakage from the euphotic zone.

5. Conclusions

The present analysis provides strong field data support for a general balance of phytoplankton growth and grazing processes in the euphotic zone of the HNLC equatorial Pacific. Instantaneous rate determinations for the depth-integrated euphotic zone from cruises in 2004 and 2005 show a mean zero net rate for

community growth minus grazing losses to micro- and mesozooplankton (Table 1). Phytoplankton production rates from experimentally determined growth rates and complementary biomass assessments at 30 stations similarly show a well-constrained balance with euphotic zone grazing losses for the community and major phytoplankton taxa. These results do not preclude a continuous rain of direct sinking export of phytoplankton from the euphotic zone, but they place reasonable limits on the flux magnitude and suggest that the mechanisms may also be local or episodic. Exactly how and where such export occurs, and how important it is in the overall budget of production, recycling and export of carbon and associated nutrients in the equatorial Pacific are important and open questions. Studies that follow and quantify the fates of production in tropical instability waves and convergence zones are likely to yield important new insights about the magnitude and mechanisms of carbon export in the equatorial Pacific.

Acknowledgments

We gratefully acknowledge the professionalism and good company of the captain and crew of the R/V *Roger Revelle*, whose efforts greatly supported this research. We especially thank Chief Scientist, David Nelson, for his open mind and thoughtful coordination of shipboard activities, and all of the many colleagues who helped with shipboard sampling and data processing. This analysis was supported in part by National Science Foundation Grants OCE 0322074, O324666 and 0417616.

References

- Allredge, A.L., Jackson, G.A., 1995. Aggregation in marine systems. *Deep-Sea Research II* 42, 1–7.
- Archer, D., Aiken, J., Balch, W., Barber, D., Dunne, J., Flament, P., Gardner, W., Garside, C., Goyet, C., Johnson, E., Kirchman, D., McPhaden, M., Newton, J., Peltzer, E., Welling, L., White, J., Yoder, J., 1997. A meeting place of great ocean currents: shipboard observations of a convergent front at 2°N in the Pacific. *Deep-Sea Research II* 44, 1827–1849.
- Balch, W.M., Drapeau, D., Fritz, J., 2000. Monsoonal forcing of calcification in the Arabian Sea. *Deep-Sea Research II* 47, 1301–1337.
- Balch, W.M., Plueddemann, A.J., Bowler, B.C., Drapeau, D.T., 2009. Chalk-Ex—fate of CaCO₃ particles in the mixed layer: evolution of patch optical properties. *Journal of Geophysical Research* 114 (C07020). doi:10.1029/2008JC004902.
- Balch, W.M., Poulton, A.J., Drapeau, D.T., Bowler, B.C., Windecker, L.A., Booth, E.S., 2011. Zonal and meridional patterns of phytoplankton biomass and carbon fixation in the equatorial Pacific Ocean between 110°W and 140°W. *Deep-Sea Research II* 58 (3–4), 400–416.
- Baudoux, A.-C., Veldhuis, M.J.W., Witte, H.J., Brussaard, C.P.D., 2007. Viruses as mortality agents of picophytoplankton in the deep chlorophyll maximum layer during IRONAGES III. *Limnology and Oceanography* 52, 2519–2529.
- Bidle, K.D., Falkowski, P., 2004. Cell death in planktonic, photosynthetic microorganisms. *Nature Reviews: Microbiology* 2, 643–655.
- Bidigare, R.R., Van Heukelem, L., Treas, C.C., 2005. Analysis of algal pigments by high performance liquid chromatography. In: Andersen, R.A. (Ed.), *Algal Culturing Techniques*. Academic Press, New York, pp. 327–345.
- Coale, K.H., Fitzwater, S.E., Gordon, R.M., Johnson, K.S., Barber, R.T., 1996a. Iron limits new production and community growth in the Equatorial Pacific Ocean. *Nature* 379, 621–624.
- Coale, K.H., Johnson, K.S., Fitzwater, S.E., Gordon, R.M., Tanner, S., Chavez, F.P., Ferioli, L., Sakamoto, C., Rogers, P., Millero, F., Steinberg, P., Nightingale, P., Cooper, D., Cochlan, W.P., Landry, M.R., Constantinou, J., Rollwagen, G., Trasvina, A., Kudela, R., 1996b. A massive phytoplankton bloom induced by an ecosystem-scale iron fertilization experiment in the equatorial Pacific Ocean. *Nature* 383, 495–501.
- Décima, M., Landry, M.R., Rykaczewski, R., 2011. Broad-scale patterns in mesozooplankton biomass and grazing in the Eastern Equatorial Pacific. *Deep-Sea Research II* 58 (3–4), 387–399.
- Dickson, M.-L., Orchoy, J., Barber, R.T., Marra, J., McCarthy, J.J., Sambrotto, R., 2001. Production and respiration rates in the Arabian Sea during 1995 Northeast and Southwest Monsoons. *Deep-Sea Research II* 48, 1199–1230.
- Dugdale, R.C., Wilkerson, F.P., 1998. Silicate regulation of new production in the Equatorial Pacific upwelling. *Nature* 391, 270–273.
- Dugdale, R.C., Wilkerson, F.P., Minas, H.J., 1995. The role of a silicate pump in driving new production. *Deep-Sea Research I* 42, 697–719.
- Dugdale, R.C., Wilkerson, F.P., Chai, F., Feely, R., 2007. Size-fractionated nitrogen uptake measurements in the equatorial Pacific and confirmation of the low Si-high-nitrate-low-chlorophyll condition. *Global Biogeochemical Cycles* 21, GB2, 005. doi:10.1029/2006GB002722.
- Dugdale, R.C., Chai, F., Feely, R.A., Measures, C.I., Parker, A.E., Wilkerson, F.P., 2011. The regulation of equatorial Pacific new production and pCO₂ by silicate-limited diatoms. *Deep-Sea Research II* 58 (3–4), 477–492.
- Franklin, D.J., Brussaard, C.P.D., Berges, J.A., 2006. What is the role and nature of programmed cell death in phytoplankton ecology? *European Journal of Phycology* 41, 1–14.
- Frost, B.W., Franzen, N.C., 1992. Grazing and iron limitation in the control of phytoplankton stock and nutrient concentration: a chemostat analogue of the Pacific equatorial upwelling zone. *Marine Ecology Progress Series* 83, 291–303.
- Garrison, D.L., Gowing, M.M., Hughes, Margaret P., Campbell, L., Caron, D.A., Dennett, M.R., Shalapyonok, A., Olson, R.J., Landry, M.R., Brown, S.L., Liu, H., Azam, F., Steward, G.F., Ducklow, H.W., Smith, D.C., 2000. Microbial food web structure in the Arabian Sea: a US JGOFS study. *Deep-Sea Research II* 47, 1387–1422.
- Kleppel, G.S., Pieper, R.E., 1984. Phytoplankton pigments in the gut contents of planktonic copepods from coastal waters off southern California. *Marine Biology* 78, 193–198.
- Jackson, G.A., 1990. A model of the formation of marine algal flocs by physical coagulation processes. *Deep-Sea Research* 37, 1197–1211.
- Johnson, K.S., Coale, K.H., Elrod, V.A., Tindale, N.W., 1994. Iron photochemistry in seawater from the equatorial Pacific. *Marine Chemistry* 46, 319–334.
- Landry, M.R., 2009. Grazing processes and secondary production in the Arabian Sea: a simple food web synthesis with measurement constraints. In: Wiggert, J.D., Hood, R.R., Naqvi, S.W.A., Brink, K.H., Smith, S.L. (Eds.), *Indian Ocean Biogeochemical Processes and Ecological Variability*. AGU Monograph. American Geophysical Union, pp. 113–146.
- Landry, M.R., Haas, L.W., Fagerness, V.L., 1984. Dynamics of microplankton communities: experiments in Kaneohe Bay, Hawaii. *Marine Ecology Progress Series* 16, 127–133.
- Landry, M.R., Constantinou, J., Kirshtein, J., 1995a. Microzooplankton grazing in the central equatorial Pacific during February and August, 1992. *Deep-Sea Research II* 42, 657–671.
- Landry, M.R., Kirshtein, J., Constantinou, J., 1995b. A refined FLB-dilution approach for measuring the community grazing impact of microzooplankton, with experimental tests in the equatorial Pacific. *Marine Ecology Progress Series* 120, 53–63.
- Landry, M.R., Barber, R.T., Bidigare, R.R., Chai, F., Coale, K.H., Dam, H.G., Lewis, M.R., Lindley, S.T., McCarthy, J.J., Roman, M.R., Stoecker, D.K., Verity, P.G., White, J.R., 1997. Iron and grazing constraints on primary production in the central equatorial Pacific: an EqPac synthesis. *Limnology and Oceanography* 42, 405–418.
- Landry, M.R., Constantinou, J., Latasa, M., Brown, S.L., Bidigare, R.R., Ondrusek, M.E., 2000. Biological response to iron fertilization in the eastern equatorial Pacific (IronEx II). III. Dynamics of phytoplankton growth and microzooplankton grazing. *Marine Ecology Progress Series* 201, 57–72.
- Landry, M.R., Brown, S.L., Neveux, J., Dupouy, C., Blanchot, J., Christensen, S., Bidigare, R.R., 2003. Phytoplankton growth and microzooplankton grazing in HNLC waters of the equatorial Pacific: community and taxon-specific rate assessments from pigment and flow cytometric analyses. *Journal of Geophysical Research* 108 (C12), 8142. doi:10.1029/2000JC000744.
- Landry, M.R., Brown, S.L., Rii, Y.M., Selph, K.E., Bidigare, R.R., Yang, E.J., Simmons, M.P., 2008. Depth-stratified phytoplankton dynamics in Cyclone *Opal*, a subtropical mesoscale eddy. *Deep-Sea Research II* 55, 1348–1359.
- Landry, M.R., Ohman, M.D., Goericke, R., Stukel, M.R., Tsyrklevich, K., 2009. Lagrangian studies of phytoplankton growth and grazing relationships in a coastal upwelling ecosystem off Southern California. *Progress in Oceanography* 53, 208–216.
- Landry, M.R., Selph, K.E., Yang, E.J., Decoupled phytoplankton growth and microzooplankton grazing in the deep euphotic zone of the HNLC equatorial Pacific. *Marine Ecology Progress Series*, in press [doi:10.3354/meps08792].
- Latasa, M., Landry, M.R., Schüller, L., Bidigare, R.R., 1997. Pigment-specific growth and grazing rates of phytoplankton in the central equatorial Pacific. *Limnology and Oceanography* 42, 289–298.
- LeBorgne, R., Landry, M.R., 2003. EBENE: a JGOFS investigation of plankton variability and trophic interactions in the equatorial Pacific (180°). *Journal of Geophysical Research* 108 (C12), 8136. doi:10.1029/2000JC001252.
- Marchetti, A., Parker, M.P., Moccia, L.P., Lin, E.O., Arrieta, A.I., Ribalet, F., Murphy, M.E.P., Maldonado, M.T., Armbrust, E.V., 2009. Ferritin is used for iron storage in bloom-forming marine pennate diatoms. *Nature* 457, 467–470.
- Menden-Deuer, S., Lessard, E.J., 2000. Carbon to volume relationships for dinoflagellates, diatoms, and other protist plankton. *Limnology and Oceanography* 45, 569–579.
- Morel, F.M.M., Rueter, J.G., Price, N.M., 1991. Iron nutrition of phytoplankton and its possible importance in the ecology of open ocean regions with high nutrient and low biomass. *Oceanography* 4, 56–61.
- Putt, M., Stoecker, D.K., 1989. An experimentally determined carbon: volume ratio for marine “oligotrichous” ciliates from estuarine and coastal waters. *Limnology and Oceanography* 34, 1097–1103.
- Richardson, T.L., Jackson, G.A., 2007. Small phytoplankton and carbon export from the surface ocean. *Science* 315, 838–840.

- Richardson, T.L., Jackson, G.A., Ducklow, H.W., Roman, M.R., 2004. Carbon fluxes through food webs of the eastern equatorial Pacific: an inverse approach. *Deep-Sea Research I* 51, 1245–1274.
- Richardson, T.L., Jackson, G.A., Ducklow, H.W., Roman, M.R., 2006. Spatial and seasonal patterns of carbon cycling through planktonic food webs of the Arabian Sea determined by inverse analysis. *Deep-Sea Research II* 53, 555–575.
- Sanderson, M.P., Hunter, C.N., Fitzwater, S.F., Gordon, R.M., Barber, R.T., 1995. Primary productivity and trace-metal contamination measurements from a clean rosette system versus ultra-clean Go-Flo bottles. *Deep-Sea Research II* 42, 431–440.
- Scheinberg, R.D., Landry, M.R., Calbet, A., 2005. Grazing impacts of two common appendicularians on the natural prey assemblage of a subtropical coastal ecosystem. *Marine Ecology Progress Series* 294, 201–212.
- Selph, K.E., Landry, M.R., Taylor, A.G., Yang, E.-J., Measures, C.I., Yang, J.J., Stukel, M.R., Christensen, S., Bidigare, R.R., 2011. Spatially-resolved taxon-specific phytoplankton production and grazing dynamics in relation to iron distributions in the Equatorial Pacific between 110 and 140°W. *Deep-Sea Research II* 58 (3–4), 358–377.
- Sherr, E.B., Sherr, B.F., 1993. Preservation and storage of samples for enumeration of heterotrophic protists. In: Kemp, P.F., Cole, J.J., Sherr, B.F., Sherr, E.B. (Eds.), *Handbook of Methods in Aquatic Microbial Ecology*. CRC Press, Boca Raton, Florida, pp. 207–212.
- Sherr, E.B., Sherr, B.F., 2007. Heterotrophic dinoflagellates: a significant component of microzooplankton biomass and major grazers of diatoms in the sea. *Marine Ecology Progress Series* 352, 187–197.
- Smith, C.R., Hoover, D.J., Doan, S.E., Pope, R.H., DeMaster, D.J., Dobbs, F.C., Altabet, M.A., 1996. Phytodetritus at the abyssal seafloor across 10° of latitude in the central equatorial Pacific. *Deep-Sea Research II* 43, 1309–1338.
- Strickland, J.D.H., Parsons, T.R., 1972. *A Practical Handbook of Seawater Analysis*. Fisheries Research Board of Canada, Ottawa.
- Strom, S.L., Miller, C.B., Frost, B.W., 2000. What sets lower limits to phytoplankton stocks in high-nitrate, low-chlorophyll regions of the open ocean? *Marine Ecology Progress Series* 193 19–31.
- Stukel, M.R., Landry, M.R., Selph, K.E., 2011. Nanoplankton mixotrophy in the eastern equatorial Pacific. *Deep-Sea Research II* 58 (3–4), 378–386.
- Taylor, A.G., Landry, M.R., Selph, K.E., Yang, E.J., 2011. Biomass, size structure and depth distributions of the microbial community in the eastern equatorial Pacific. *Deep-Sea Research II* 58 (3–4), 342–357.
- Vaulot, D., Marie, D., Olson, R.J., Chisholm, S.W., 1995. Growth of *Prochlorococcus*, a photosynthetic prokaryote, in the equatorial Pacific Ocean. *Science* 268, 1480–1482.
- Verity, P.G., Langdon, C., 1984. Relationship between lorica volume, carbon, nitrogen, and ATP content of tintinnids in Narragansett Bay. *Journal of Plankton Research* 6, 859–868.
- Verity, P.G., Stoecker, D.K., Sieracki, M.E., Nelson, J.R., 1996. Microzooplankton grazing of primary production at 140°W in the equatorial Pacific. *Deep-Sea Research II* 43, 1227–1255.
- Yoder, J.A., Ackelson, S.G., Barber, R.T., Flament, P., Balch, W.M., 1994. A line in the sea. *Nature* 371, 689–693.
- Zhang, X., Dam, H.G., White, J.R., Roman, M.R., 1995. Latitudinal variations in mesozooplankton grazing and metabolism in the central tropical Pacific during the US JGOFS EqPac Study. *Deep-Sea Research II* 42, 695–714.